Robust, FFT-Based, Block Demodulation in the Presence of Symbol Synchronization Jitter, Using Symmetric, Differential, Phase Shift, Keying (SDPSK)

by

Ahmad A. Masoud

Suite 12A, 71Brock St., Kingston, Ontario K7L 1R8, Canada, E-mail: Masoud@host.king.igs.net

Aziz G. Qureshi

Dept. of Elec. Eng., University of Adelaide, Adelaide SA 5005, Australia, E-mail: aqureshi@eleceng.adelaide.edu.au

Abstract

In this paper a new binary differential phase encoding technique is suggested. The suggested approach, Symmetric Differential Phase Shift Keying (SDPSK), is designed to alleviate the symbol synchronization difficulties which optimum DPSK may encounter while maintaining the same PE in the absence of time jitter. Also an economical and compact Fast Fourier Transform (FFT) - based realization of the block demodulators for both optimum DPSK and SDPSK encoded signals is suggested. Theoretical developments along with simulation results are provided.

1. Introduction

This paper describes a new modulation technique along with the corresponding block demodulator that is suitable for use in situations that place stringent requirements on the ability of the receiver to reliably synchronize the symbols. To address the signal acquisition reliability requirements, differential phase encoding techniques are used. Such techniques do not require carrier synchronization (i.e. noncoherent). In particular, a differential phase encoding technique that is named Symmetric, Differential, Phase, Shift Keying (SDPSK) is proposed for modulation. This method of differential phase encoding is expected to provide high symbol synchronization reliability. It is shown that in the absence of time jitter SDPSK has the same Probability of Error (PE) as the optimum DPSK [1,2] with the added advantage of high resistance to Symbol Synchronization Jitter (SSJ). The optimum DPSK, and the SDPSK demodulators are realized using the Fast Fourier Transform (FFT) algorithm [3]. FFT naturally lends itself to the block-demodulation of differentially-encoded signals. Also, the availability of VLSI FFT chips makes a FFT realization of the receiver a suitable choice for a compact, economical, and a low power consumption realization. The performance of the receiver is evaluated in the presence of SSJ using simulation experiments.

2. The Suggested Modulation Method

In the following, optimum DPSK is quickly reviewed in a manner that allows for a digital implementation. Also the new modulation technique is presented.

2.1: Optimum DPSK

The block diagram describing a DPSK modulator is shown in Figure-1 below :

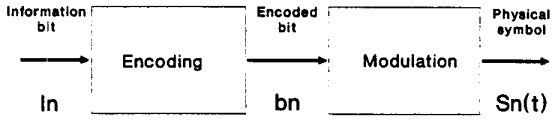

Figure-1 : Block diagram of a DPSK modulator.

An information bit I_n can only assume a value from the binary set {0,1}. Prior to modulation I_n is first encoded. The encoded bit b_n is generated using the formula

$$b_n = b_{n-1} \oplus I_n , \qquad (1)$$

$\oplus$ is the logical XOR operation, and $b_0 = 1$. The Physical symbol which is transmitted through the channel ($S_n(t)$) belongs to the antipodal set of signals {S1(t),S2(t)} where

$$S1(t) = A\cdot COS(\omega t),$$

and $$S2(t) = A\cdot COS(\omega t + \pi) = - A\cdot COS(\omega t), \quad t \in [0,T), \qquad (2)$$

where A is the amplitude of the carrier, and T is its duration. The symbols to be transmitted are selected as follows :

$$\text{if } b_n = 1, \ S_n(t) = S1(t), \qquad \text{if } b_n = 0, \ S_n(t) = S2(t) \qquad (3)$$

It can be easily shown that if $I_n=1$, $S_n(t) = S_{n-1}(t)$. On the other hand if $I_n=0$, $S_n(t) = -S_{n-1}(t)$. Decoding of a DPSK signal is based on this property.

2.2 A DPSK Receiver:

Let $\hat{S}_n(t)$ and $\hat{S}_n(i)$ be the n'th symbol received from the channel, and the digitized symbol respectively, where i is the time index and the sampling rate ($f_s = (1\backslash \Delta T)$, $N\cdot\Delta T = T$), i=0,..,N-1, (Figure-2) .

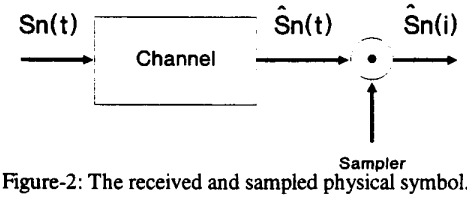

Figure-2: The received and sampled physical symbol.

Let η_n be a 2-D phasor vector describing the n'th received symbol ($\eta_n = [\ \eta c_n \ \ \eta s_n\ ]^t$), where

$$\eta c_n = \sum_{i=1}^{N-1} \hat{S}_n(i) \cdot COS\left(\frac{\omega T}{N} i\right), \qquad \text{and}$$

$$\eta c_n = \sum_{i=1}^{N-1} \hat{S}_n(i) \cdot SIN\left(\frac{\omega T}{N} i\right). \qquad (4)$$

To make a decision regarding the n'th received bit, the following decision variable needs to be constructed:

$$\gamma_n = \eta_n^t \ \eta_{n-1} = \eta c_n \ \eta c_{n-1} + \eta s_n \ \eta s_{n-1} . \qquad (5)$$

If $\gamma_n \geq 0$, then a decision is made that $I_n = 1$ was transmitted. Otherwise a decision is made that $I_n = 0$ was transmitted.

DPSK may face a problem when long runs of the same bit are encountered. For example:

n	1	2	3	4	5	6	7	8
I_n	1	1	1	1	1	1	1	1
b_n	1	1	1	1	1	1	1	1
S_n	S1	S1	S1	S1	S1	S1	S1	S1 .

Such a situations places high strain on the symbol synchronization circuitry. The difficulty is encountered due to the lack of a fundamental

0-7803-5284-X/99/$10.00 © 1999 IEEE.

frequency component with a period T in the spectrum of the received signal. This makes it difficult to accurately determine the beginning and end of a symbol.

2.3 SDPSK:

A new form of differential phase encoding called Symmetric Differential Phase Shift Keying (SDPSK) is suggested to circumvent the difficulties encountered by DPSK. Instead of using an antipodal set of symbols, as in DPSK, to modulate the information bits, SDPSK uses an orthogonal set of four symbols in the modulation process to make sure that no two successive symbols are alike. The symbols used by SDPSK are:

$$S0(t) = A\cdot COS(\omega t),$$
$$S1(t) = A\cdot COS(\omega t + \pi/2) = A\cdot SIN(\omega t),$$
$$S2(t) = A\cdot COS(\omega t + \pi) = -A\cdot COS(\omega t),$$
and $$S3(t) = A\cdot COS(\omega t + 3\pi/2) = -A\cdot SIN(\omega t). \quad (6)$$

The above symbols may be viewed as a constellation of four phasor vectors situated at a right angle to each other. The transmitted physical symbol $S_n(t)$ may be seen as a phasor vector that assumes the position of any of the four phasors above. Encoding an information bit is carried out by rotating the phasor $S_n(t)$ counter-clock-wise if $I_n=1$, and clock-wise if $I_n=0$, or simply

$$S_n(t) = A \cdot COS\ (\omega t + \frac{\pi}{2} \cdot a_n)\ , \quad (7)$$

where $a_n = a_n - 1$, for $I_n = 0$, and $a_n = a_n + 1$, for $I_n = 1$, $a_0 = 0$. .

2.4 A SDPSK Receiver:

Similar to DPSK, decoding a SDPSK signal starts by constructing the phase vector η_n. Since the direction of rotation of the phasor determines the information bit that was transmitted, the decision variable is constructed as follows:

$$\gamma_n = \eta_n \times \eta_{n-1} = \eta c_n\ \eta s_{n-1} - \eta s_n\ \eta c_{n-1}\ . \quad (8)$$

If $\gamma_n \geq 0$, then a decision is made that $I_n = 1$ was transmitted. Otherwise a decision is made that $I_n = 0$ was transmitted.

Since SDPSK encodes information by continuously rotating the phasor, no two successive symbols are alike regardless of the statistical distribution of the information bits. For example:

n	1	2	3	4	5	6	7	8
I_n	1	1	1	1	1	1	1	1
S_n	S0	S1	S2	S3	S0	S1	S2	S3 .

As can be seen in a SDPSK encoded signal a component having the fundamental frequency of 1/T will always be present in the received signal enabling the synchronizing circuitry, at all times, to determine the beginning and end of a symbol.

3.0 Frequency Domain Multi-Channel Coding

In the above approach, each symbol the modulator transmits into the channel carries the informational equivalence of one bit only (Figure-3).

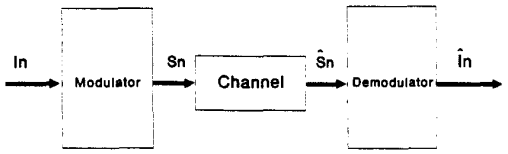

Figure-3: A symbol encoding one information bit only.

In essence a physical symbol is a vehicle for transmitting information through a physical channel. A symbol has a capacity for carrying information which may be underutilized by restricting its informational content to one information bit only. This capacity is better utilized by encoding more than one information bit in the symbol (Figure-4).

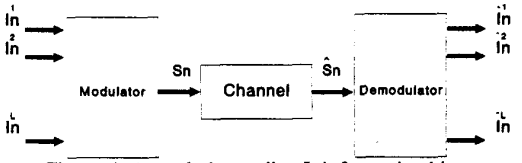

Figure-4: A symbol encoding L information bits.

One way to synthesize a symbol with an informational equivalence of L information bits (from now on, information bits will be referred to as channels) is to assign to each channel a set of symbols that is orthogonal to the other sets used for modulating bits from the other channels, i.e.

$$\{S1^1,..,SM^1\} \perp \{S1^2,..,SM^2\} \perp .....\perp \{S1^L,..,SM^L\}\ , (9)$$

$$\sum_{i=0}^{N-1} S_l^k(i)\ S_j^m(i) \equiv 0 \qquad \forall\ k=1,..,L\ ,\ m=1,..,L\ ,\ k\neq m$$
$$l=1,..,M\ ,\ j=1,..,M\ ,$$

where M is the number of basis symbols in each set. Since for DPSK and SDPSK sinusoidal signals are used, building basis symbols can be easily carried out using

$$S_j^k(i) = A \cdot COS(\frac{\omega_k T}{N} i + \phi j)\ , \quad (10)$$

$$\sum_{i=0}^{N-1} A\cdot COS(\frac{\omega_k T}{N} i + \phi j)\ A\cdot COS(\frac{\omega_m T}{N} i + \phi l) \equiv 0\ .$$

The above condition is satisfied if ω_k and ω_m are chosen as

$$\omega_k = \frac{2\pi}{T} k\ ,\quad \omega_m = \frac{2\pi}{T} m\ . \quad (11)$$

Therefore, a discrete basis symbol has the form:

$$S_j^k(i) = A \cdot COS(\frac{2\pi}{N} k\, i + \phi j)\ , \quad (12)$$

or for the continuous time case

$$S_j^k(t) = A \cdot COS(\frac{2\pi}{T} k\, t + \phi j)\ .$$

In other words, for orthogonality, the frequency of a symbol must be chosen so that it produces an integer number of cycles within one symbol duration.

3.1 Informational Capacity of a Symbol:

In order to determine the number of channels that can be encoded in one symbol, the transmitted signal is assumed to be frequency limited to a bandwidth of BW. Also it is assumed that the Nyquest rate is used to sample the signal, i.e. $f_s = 2\cdot BW$. The highest frequency of a basis symbol is assumed to be equal to that of bandwidth (BW)

$$\omega_{k_{max}} = \frac{2\pi}{T} k_{max} = 2\cdot\pi\cdot BW\ . \quad (13)$$

Therefore, $$k_{max} = \frac{T\cdot fs}{2} = \frac{T}{2\cdot\Delta T} = \frac{N}{2}\ . \quad (14)$$

In other words, a symbol can carry at most N/2 channels. This is an optimistic estimate that can only hold in the absence of SSJ. Once a symbol is disturbed by this artifact power from individual channels leaks disturbing the operation of the channels and bringing up the Probability of Error (PE). In other words the channels are no longer orthogonal. In this case the channels can not be tightly packed and guard bands between them should be placed to minimize the interference; hence reduce the informational capacity of the symbol. A symbol carrying more than one information bit has the form:

$$S_n(t) = A\cdot[COS(\omega_1 t + \phi_n^1) + ... + COS(\omega_L t + \phi_n^L)]\ , \quad (15)$$

where the ϕ's encode the information bits from the channels.

4.0 FFT-Based Block Demodulation of DPSK and SDPSK Encoded Signals

In this section a procedure utilizing the Fast Fourier Transform (FFT) algorithm is suggested for the block demodulation of the received and discritized multichannel symbol $\hat{S}_n(i)$. The Discrete Fourier Transform (DFT) of $\hat{S}_n(i)$ is defined as :

$$F_n(k) = DFT(\hat{S}_n(i)) = \sum_{i=0}^{N-1} \hat{S}_n(i)\, e^{j\frac{2\pi}{N} k i} \qquad (16)$$

$$= \sum_{i=0}^{N-1} \hat{S}_n COS(\frac{2\pi}{N} k i) + j \sum_{i=0}^{N-1} \hat{S}_n(i) SIN(\frac{2\pi}{N} k i) .$$

As can be seen the phasor vector in equation-4, which is needed to construct the decision variable for the k'th channel, is equal to the k'th component of the DFT of the received symbol, i.e.

$$\eta_n^k = F_n(k),\ \eta c_n^k = Re(F_n(k)) \ ,\ \&\ \eta s_n^k = Im(F_n(k)) \ . \qquad (17)$$

Note that FFT is only a fast implementation of DFT. The n'th bit in the k'th channel may be decoded as follows:

a. DPSK (Figure-5)

$$\gamma_n(k) = Re(F_n(k))Re(F_{n-1}(k)) + Im(F_n(k))Im(F_{n-1}(k)) \ , \qquad (18)$$

If $\gamma_n(k) \geq 0$, $I_n^k = 1$, If $\gamma_n(k) < 0$, $I_n^k = 0$.

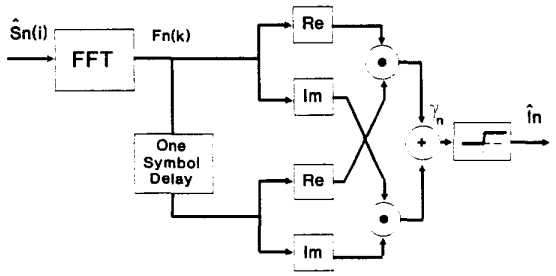

Figure-5: A DPSK, FFT-based, block demodulator, SSJ-free case.

b. SDPSK (Figure-6)

$$\gamma_n(k) = Re(F_n(k))Im(F_{n-1}(k)) - Im(F_n(k))Re(F_{n-1}(k)) \ , \qquad (19)$$

If $\gamma_n(k) \geq 0$, $I_n^k = 1$, If $\gamma_n(k) < 0$, $I_n^k = 0$.

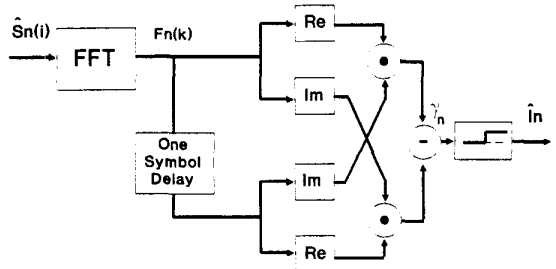

Figure-6: A SDPSK, FFT-based, block demodulator, SSJ-free case.

5.0 SSJ Effect on The Communication Link

Although SDPSK is designed with the aim of providing high immunity to SSJ, the fact remains that SSJ, if occurs, can seriously interfere with the functioning of the communication link. Therefore, the effect of SSJ must not be neglected even if SDPSK is being used. In the following two ways in which SSJ can impact on performance are discussed.

5.1 Inter-channel Interference:

To designate a certain carrier frequency the status of a channel it should be possible to uniquely separate the informational contents of that channel from the others. Unfortunately, the presence of SSJ dramatically changes this situation. SSJ tampers with the orthogonality of the channels causing the power from the individual channels to leak. In other words, the carriers are no longer orthogonal. Figure-7a shows the power concentration from a single orthogonal carrier. Figure-7b shows the effect of SSJ on the ability of a carrier to confine its power to the frequency location that is designated for the channel.

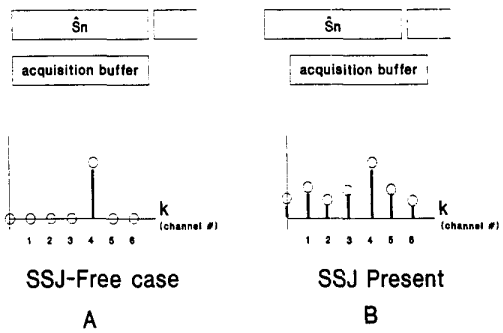

Figures-7a,b: Effect of SSJ on the power distribution of a channel.

5.2 Differential Phase Noise

The effect of SSJ on the communication link is far more intrusive than just causing Interchannel interference. SSJ also causes relative phase disturbance. By disturbing the relative phase between two successive symbols SSJ poses the threat of rendering the received signal unusable for decoding the information in its differential phase. This serious artifact arises due to the misalignment between two successively collected signals representing two successive symbols. This is a direct result of the failure of the synchronization circuitry to accurately determine the start and end of the received symbols. In the following it is shown that differential phase noise ($\Delta\theta_n^k$) unevenly affects the individual channels with the high frequency channels being more susceptible to this noise than the low frequency ones.

Let us assume that due to inaccurate localization of the beginning and end of a received symbol the n'th symbol begin registering in the collection buffer at time $t=\Delta_n \cdot T$ instead of t=0 (Figure-8). In the same way the acquisition of the n-1'th symbol begins at $t=\Delta_{n-1} \cdot T$. Both Δ_n and Δ_{n-1} are independent, uniformly distributed random variables. As can be seen from Figure-8, relative to the receiver, a random misalignment of symbol S_n relative to S_{n-1} of the amount $(\Delta_n - \Delta_{n-1}) \cdot T$ has occurred. To compute how much phase disturbance this misalignment causes in each channel, we need first to compute the one cycle duration in the k'th channel (T_k):

$$T_k = \frac{T}{k} \ . \qquad (20)$$

Since one cycle duration in a channel corresponds to a 2π phase relative to that channel, the misalignment causes the following differential phase shift in the k'th channel:

$$\Delta\theta_n^k = 2\pi \cdot \frac{\Delta_n - \Delta_{n-1}}{T_k} T = 2\pi \cdot (\Delta_n - \Delta_{n-1})\, k \ . \qquad (21)$$

As can be seen, differential phase noise intensifies as the frequency of a channel goes up.

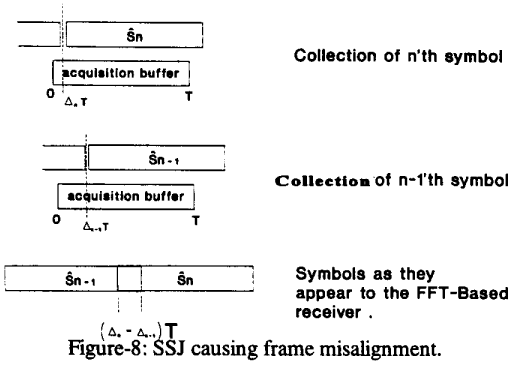

Figure-8: SSJ causing frame misalignment.

In the next section counter measures to alleviate the leakage effect are described. Also the structure of the FFT-Based Block demodulator is adjusted to eliminate the differential phase noise which SSJ introduces.

6.0 SSJ Countermeasures

The followings are measures to counteract the effect of SSJ:

6.1 Removing Differential Phase Noise:

The most serious SSJ-induced artifact is the differential phase noise. To show the severity of this artifact, a two-channel (k=1,7), 16-sample, DPSK block receiver that is constructed using the procedure in section-2 is simulated. Table-1 shows the PE computed over 200,000 transmissions at medium levels of noise (i.e. Eb/No) for the SSJ-free case and a small value of SSJ. As can be seen for the SSJ-free case, PE is the same for both the high and low frequency channels. However, The situation dramatically changes when little SSJ is introduced. While the low frequency channel suffers some degradation in performance, the high frequency channel performance suffers serious degradation rendering the channel unusable for transmitting information.

Jitter	Eb/No	Pe k=1	Pe k=7
0.00%	6.25	0.0010	0.0010
0.00%	4.00	0.0088	0.0085
6.25%	6.25	0.0093	0.4990
6.25%	4.00	0.0414	0.5070

Table-1: Effect of SSJ on PE, 2-channel, 16 sample, DPSK.

Fortunately, SSJ-induced differential phase noise can be totally eliminated by slightly modifying the FFT-Based receiver in section-2. The idea is simple, instead of restricting the acquisition buffer to the duration of one symbol only, it is made large enough to accommodate two symbols (Figure-9).

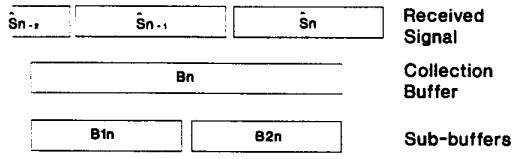

Figure-9: An approach to eliminate frame misalignment.

The signal in the collection buffer is then splitted into two sub-buffers each having the duration of one symbol only. This arrangement makes sure that no misalignment between the n'th and n-1'th symbol can occur causing the differential phase noise. The new procedure for decoding the n'th symbol is:

1- acquire the signal $B_n(i)$, i=0,...,2N-1 ,

2- construct the following signals

$$B1_n(j) = B_n(j) \qquad j=0,..,N-1 \qquad (22)$$
$$B2_n(j) = B_n(j+N) ,$$

3- compute

$$F1_n(k) = FFT(B1_n(j)) , \text{ and} \qquad (23)$$
$$F2_n(k) = FFT(B2_n(j)) ,$$

4- in case of a DPSK signal (Figure-10)

$$\gamma_n(k) = Re(F1_n(k))Re(F2_n(k)) + Im(F1_n(k))Im(F2_n(k)) \quad , \quad (24)$$

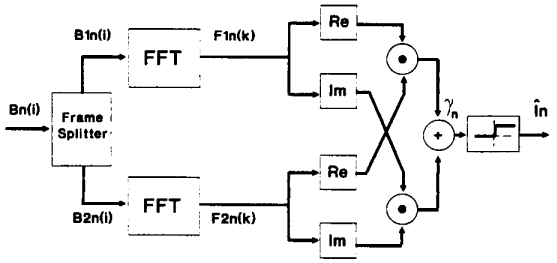

Figure-10: SSJ resistant, FFT-based, DPSK, demodulator.

5- in case of a SDPSK signal (Figure-11)

$$\gamma_n(k) = Re(F1_n(k))Im(F2_n(k)) - Im(F1_n(k))Re(F2_n(k)) \quad , \quad (25)$$

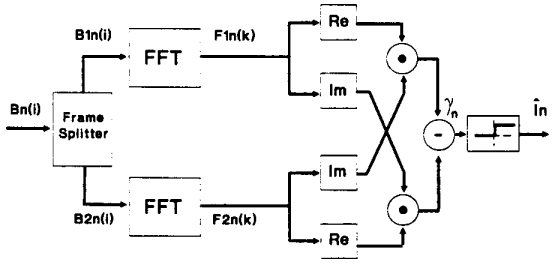

Figure-11: SSJ resistant, FFT-based, SDPSK, demodulator.

6- if $\gamma_n(k) \geq 0$, $I_n^k=1$, If $\gamma_n(k) < 0$, $I_n^k=0$. (26)

As can be seen, eliminating SSJ-induced differential phase noise is carried out at the expense of slightly increasing the computational effort that is needed to decode one symbol. In The SSJ-resistant receiver two FFTs are needed to decode one symbol instead of one as in the SSJ-free case. Since both FFTs are executed in parallel, the receiver experiences no slow down in operation.

6.2 Reducing Inter-channel Interference by windowing:

Reducing the SSJ-induced channel leakage may be achieved by reducing the importance of the peripheral samples of the data in the sub-buffers. One way for accomplishing this is by multiplying the data in the sub-buffers with a proper window function [4] prior to performing FFT. This can significantly confine the leak of power from the individual channels and significantly reduce PE. Unfortunately, windowing has minor disadvantages which are, never-the-less, outweighed by the improvement it introduces. First, windowing leads to a loss in the signal power; second, and more important, in containing channel leakage, windowing tends to concentrate the power in the neighborhood of that channel (this is controlled by the mainlobe width of the window). Although interference with distant channels (this is controlled by the side lobe level of the window) is reduced, interference with adjacent channels increases. Therefore, the selection of a window function has to be carefully carried out so that PE may be reduced.

7.0 PE, SSJ-Free Case

In the following approximate formulae and exact expressions for the probabilities of error for both DPSK and SDPSK receivers are derived for the SSJ-free case. It is shown that PEs for both receivers are identical. First, the following two results are needed. Unfortunately, due to limitation on space only the statements of the results are provided with no proofs:

1- the signal to noise ratio (Eb/No) expressed as a function of the number of samples per symbol duration (N), the variance of the noise samples (σ_n^2), and the magnitude of the carrier (A) is:

$$\frac{E_b}{N_o} = \frac{A^2 N}{4\,\sigma_n^2} . \tag{27}$$

2- the samples of a Band-limited, White, Guassian, Noise taken at the Nyquest rate are independent.

7.1 PE-DPSK, Guassian Approximation:

In this section an approximate expression for the probability of error for a DPSK receiver in the absence of SSJ is derived. First the probability distribution of both ηc_n & ηs_n is determined.

$$\eta c_n = \sum_{i=0}^{N-1} \hat{S}_n(i)\, cos(\frac{\omega_k T}{N} i) \tag{28}$$

$$= \sum_{i=0}^{N-1} [A\, cos(\frac{\omega_k T}{N} i + \phi_n + \theta) + n(i)\,]\, cos(\frac{\omega_k T}{N} i)$$

$$= A\, cos(\phi_n + \theta) \sum_{i=0}^{N-1} cos^2(\frac{\omega_k T}{N} i)$$

$$- A\, sin(\phi_n + \theta) \sum_{i=0}^{N-1} cos(\frac{\omega_k T}{N} i)\, sin(\frac{\omega_k T}{N} i)$$

$$+ \sum_{i=0}^{N-1} cos(\frac{\omega_k T}{N} i)\, n(i)$$

$$= \frac{A N}{2} cos(\phi_n + \theta) + \sum_{i=0}^{N-1} cos(\frac{\omega_k T}{N} i)\, n(i) .$$

As can be seen ηc_n, is a guassian r.v. With mean:

$$mc_n = \frac{A N}{2} cos(\phi_n + \theta) , \tag{29}$$

and variance

$$\sigma c_n^2 = \sigma_n^2 \sum_{i=0}^{N-1} cos^2(\frac{\omega_k T}{N} i) = \frac{N}{2}\sigma_n^2 .$$

As for the quadrature component, we have

$$\eta s_n = \sum_{i=0}^{N-1} \hat{S}_n(i)\, sin(\frac{\omega_k T}{N} i) \tag{30}$$

$$= \sum_{i=0}^{N-1} [A\, cos(\frac{\omega_k T}{N} i + \phi_n + \theta) + n(i)]\, sin(\frac{\omega_k T}{N} i)$$

$$= A\, cos(\phi_n + \theta) \sum_{i=0}^{N-1} cos(\frac{\omega_k T}{N} i)\, sin(\frac{\omega_k T}{N} i)$$

$$- A\, sin(\phi_n + \theta) \sum_{i=0}^{N-1} sin^2(\frac{\omega_k T}{N} i)$$

$$+ \sum_{i=0}^{N-1} sin(\frac{\omega_k T}{N} i)\, n(i)$$

$$= -\frac{A N}{2} sin(\phi_n + \theta) + \sum_{i=0}^{N-1} sin(\frac{\omega_k T}{N} i) n(i) .$$

As can be seen ηs_n, is a guassian r.v. With mean

$$ms_n = -\frac{A N}{2} sin(\phi_n + \theta) , \tag{31}$$

and variance

$$\sigma s_n^2 = \sigma_n^2 \sum_{i=0}^{N-1} sin^2(\frac{\omega_k T}{N} i) = \frac{N}{2}\sigma_n^2 .$$

The decision variable γ_n consists of the sum:

$$\gamma_n = \gamma 1_n + \gamma 2_n , \tag{32}$$

where

$$\gamma 1_n = \eta c_n \cdot \eta c_{n-1} ,$$
$$\gamma 2_n = \eta s_n \cdot \eta s_{n-1} .$$

It was shown in [5] that the PDF of the product of two independent guassian rvs with means m_a and m_b, and variances σ_a^2 & σ_b^2 may be approximated with a guassian rv that has the mean

$$m = m_a\, m_b , \tag{33}$$

and variance $\sigma^2 = \sigma_a^2\, \sigma_b^2 + m_a^2\, \sigma_b^2 + m_b^2\, \sigma_a^2$.

Therefore, $\gamma 1_n$ has a guassian PDF with a mean

$$m_1 = \frac{A^2 N^2}{4} cos(\phi_n + \theta)\, cos(\phi_{n-1} + \theta) , \tag{34}$$

and variance

$$\sigma_1^2 = \frac{N^2}{4}\sigma_n^4 + \frac{A^2 N^3}{8}\sigma_n^2 [cos^2(\phi_n + \theta) + cos^2(\phi_{n-1} + \theta)] . \tag{35}$$

In a similar way, $\gamma 2_n$ has a guassian PDF with a mean:

$$m_2 = \frac{A^2 N^2}{4} sin(\phi_n + \theta)\, sin(\phi_{n-1} + \theta) , \tag{36}$$

and variance

$$\sigma_2^2 = \frac{N^2}{4}\sigma_n^4 + \frac{A^2 N^3}{8}\sigma_n^2 [sin^2(\phi_n + \theta) + sin^2(\phi_{n-1} + \theta)] . \tag{37}$$

Since the quadrature and in-phase components of a guassian rv are independent and γ_n is the sum of two independent guassian rvs, its PDF is also guassian with mean

$$m_\gamma = (A^2 N^2/4)[cos(\phi_n + \theta) cos(\phi_{n-1} + \theta) + sin(\phi_n + \theta) sin(\phi_{n-1} + \theta)],$$

$$= \frac{A^2 N^2}{4} cos(\phi_n - \phi_{n-1}) = \begin{cases} mc & \phi_n = \phi_{n-1} \\ -mc & \phi_n \neq \phi_{n-1} \end{cases} ,$$

$$\sigma_\gamma^2=\frac{N^2}{2}\sigma_n^4+\frac{A^2N^3}{4}\sigma_n^2 . \quad (38)$$

PE for the DPSK receiver may be computed as :

$$PE=Pr(\gamma_n< 0/1)Pr(1)+Pr(\gamma_n\geq 0/0)Pr(0)$$

$$=\frac{1}{2\sqrt{2\pi}\,\sigma_v}\left[\int_{-\infty}^{0} exp(-\frac{1}{2}\frac{(x-mc)^2}{\sigma_v^2})dx+\int_{0}^{\infty} exp(-\frac{1}{2}\frac{(x-(-mc))^2}{\sigma_v^2})dx\right]$$

$$=\frac{1}{2}\left(1-erf\left(\frac{\sqrt{2}A^2N}{4\sigma_\gamma\sqrt{2\sigma_\gamma^2+A^2N}}\right)\right) \quad (39)$$

$$=\frac{1}{2}(erfc(\frac{\frac{Eb}{No}}{\sqrt{1+2\frac{Eb}{No}}}))\approx\frac{1}{2}(erfc(\sqrt{\frac{1}{2}\frac{Eb}{No}}))\ .$$

7.2 PE-SDPSK, Guassian Approximation:

For SDPSK the two components of the decision variable are:

$$\gamma 1_n = \eta c_n\cdot\eta s_{n-1}\ ,$$
$$\gamma 2_n = -\eta s_n\cdot\eta c_{n-1}\ . \quad (40)$$

Similar to the DPSK case, both variables may be approximated as guassian rvs with the following means and variances

$$m_1=-\frac{A^2N^2}{4}cos(\phi_n+\theta)sin(\phi_{n-1}+\theta)\ , \quad (41)$$

$$\sigma_1^2=\frac{N^2}{4}\sigma_n^4+\frac{A^2N^3}{8}\sigma_n^2[cos^2(\phi_n+\theta)+sin^2(\phi_{n-1}+\theta)]\ .$$

$$m_2=-\frac{A^2N^2}{4}sin(\phi_n+\theta)cos(\phi_{n-1}+\theta)\ ,$$

$$\sigma_2^2=\frac{N^2}{4}\sigma_n^4+\frac{A^2N^3}{8}\sigma_n^2[sin^2(\phi_n+\theta)+cos^2(\phi_{n-1}+\theta)]\ .$$

Since the quadrature and in-phase components of a guassian rv are independent and γ_n is the sum of two independent guassian rvs, its PDF is also guassian with mean

$$m_\gamma=-\frac{A^2N^2}{4}[cos(\phi_n+\theta)sin(\phi_{n-1}+\theta)-sin(\phi_n+\theta)cos(\phi_{n-1}+\theta)]\ ,$$

$$=\frac{A^2N^2}{4}sin(\phi_n-\phi_{n-1})=\begin{cases} mc & \phi_n-\phi_{n-1}=\frac{\pi}{2} \\ -mc & \phi_n-\phi_{n-1}=-\frac{\pi}{2}\end{cases}, \quad (42)$$

and a variance $$\sigma_\gamma^2=\frac{N^2}{2}\sigma_n^4+\frac{A^2N^3}{4}\sigma_n^2\ . \quad (43)$$

Using the above, the probability of error for the SDPSK receiver is:

$$PE=\frac{1}{2\sqrt{2\pi}\sigma_\gamma}\left[\int_{-\infty}^{0} exp(-\frac{1}{2}\frac{(x-mc)^2}{\sigma_\gamma^2})dx+\int_{0}^{\infty} exp(-\frac{1}{2}\frac{(x-(-mc))^2}{\sigma_\gamma^2})dx\right]$$

$$=\frac{1}{2}(erfc(\frac{\frac{A^2N}{4\sigma_\gamma^2}}{\sqrt{1+2\frac{A^2N}{4\sigma_\gamma^2}}}))$$

$$=\frac{1}{2}(erfc(\frac{\frac{Eb}{No}}{\sqrt{1+2\frac{Eb}{No}}}))\approx\frac{1}{2}(erfc(\sqrt{\frac{1}{2}\frac{Eb}{No}}))\ . \quad (44)$$

For the SSJ-free case, both DPSK and SDPSK have identical PEs.

7.3: Exact PE:

Due to limitation on space only the expression for the exact PE is provided below.

$$PE=\frac{1}{2}\left[\int_{-\infty}^{\infty} f1(\gamma 1,\pi,\pi)Gn(\gamma 1)+f1(\gamma 1,0,\pi)Gp(\gamma 1)\right]d\gamma 1\ ,$$

Where

$$f1(\gamma 1,\phi_n,\phi_{n-1})=\frac{1}{\pi N\sigma_n^2}\int_{-\infty}^{\infty}\frac{1}{|\omega|}e^{-\frac{1}{N\sigma_n^2}[(\omega-mc_n(\phi_n))^2+(\frac{\gamma 1}{\omega}-mc_n(\phi_{n-1}))^2]}d\omega\ .$$

$$f2(\gamma 2)=\frac{2}{\pi N\sigma_n^2}K0(2\frac{\gamma 2}{N\sigma_n^2})\ .\ ,$$

$$Gn(\gamma 1)=\int_{-\infty}^{-\gamma 1} f2(\gamma 2)\,d\gamma 2\ ,$$

and

$$Gp(\gamma 1)=\int_{-\gamma 1}^{\infty} f2(\gamma 2)\,d\gamma 2\ . \quad (45)$$

K0 is the Bessel function of the second kind of zero order.

The following table show the values of PE for the SSJ-free, DPSK case computed for different values of Eb/No using the Guassian approximation, the exact formula, and by simulation:

Eb/No	PE Guassian	PE Exact	PE Simulation
11.11	4.293e-4	6.47e-6	3.75 e-6
08.16	0.00214	0.000138	0.00012
06.25	0.00621	0.001103	0.00099
04.94	0.01312	0.003594	0.00348
04.00	0.02275	0.0094	0.00916
03.31	0.03443	0.01833	0.01802
02.79	0.04743	0.0312	0.03075

Table-2: PE, approximation, Exact, and Simulation.

As can be seen the accuracy of the Guassian approximation seriously deteriorates as Eb/No increases. On the other hand, the values of PE computed using the exact formula closely follow those obtained by simulation (see section 8).

8.0 Simulation Results

In the following preliminary simulation results of the suggested SDPSK & the DPSK receivers are presented. The receivers are required to decode the symbols of a four-channel communication link (k=1,3,5,7) using a 16-point FFT algorithm. PE is computed for different values of Eb/No by averaging the number of errors from 500,000 transmissions. Due to limitations on space, the PE tables for DPSK & SDPSK are only reported for the SSJ-free case. The results with SSJ are reported using graphs that constructed for three window functions (rectangular window (i.e no window is used), Hamming window, & Truncated Triangular window). It is obvious from tables 3 &4 that within the uncertainty created by the finite number of trails used to carry out the simulation experiments, the PEs of the DPSK & SDPSK receivers are the same.

Figures 12-17 show that the choice of a window is a significant factor that affecting performance in the presence of SSJ which has to be carefully examined.

Eb/No	Pe k=1	Pe k=3	Pe k=5	Pe k=7	Pe Mean
11.11	1.5e-005	0	0	0	3.75e-006
08.16	0.000125	0.00011	0.000155	8.5e-005	0.0001188
06.25	0.000995	0.001145	0.000915	0.00091	0.0009912
04.94	0.003705	0.00328	0.0034	0.00352	0.003476
04.00	0.009455	0.008955	0.00919	0.009045	0.009161
03.31	0.01821	0.0181	0.01777	0.01801	0.01802
02.78	0.03092	0.03054	0.03047	0.03109	0.03075

Table-3: 4-channel, DPSK, SSJ-free, no windowing.

Eb/No	Pe k=1	Pe k=3	Pe k=5	Pe k=7	Pe Mean
11.11	1.5e-005	5e-006	5e-006	5e-006	7.5e-006
08.16	0.000135	0.00018	0.000125	0.000135	0.000144
06.25	0.001	0.00083	0.000925	0.001025	0.000945
04.94	0.003635	0.00349	0.003385	0.00362	0.003533
04.00	0.008795	0.00938	0.009405	0.008495	0.009019
03.31	0.01845	0.01772	0.01821	0.01861	0.01825
02.78	0.03074	0.02951	0.03107	0.03096	0.03057

Table-4: 4-channel, SDPSK, SSJ-free, no windowing.

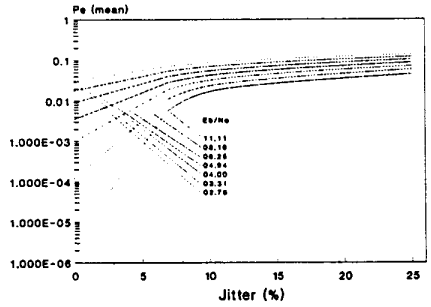

Figure-12: Mean PE, 4-Channel DPSK, Rectangular window.

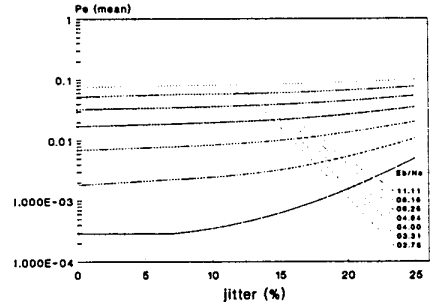

Figure-13: Mean PE, 4-Channel DPSK, Hamming window.

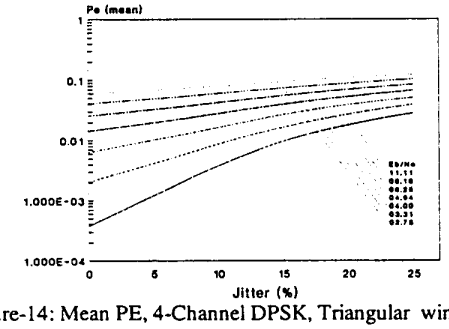

Figure-14: Mean PE, 4-Channel DPSK, Triangular window.

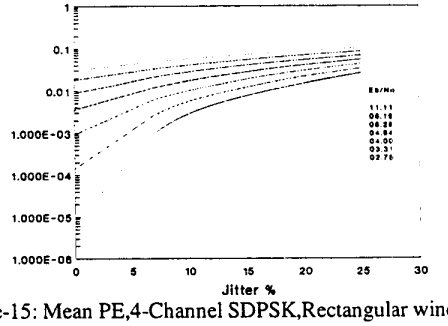

Figure-15: Mean PE,4-Channel SDPSK,Rectangular window.

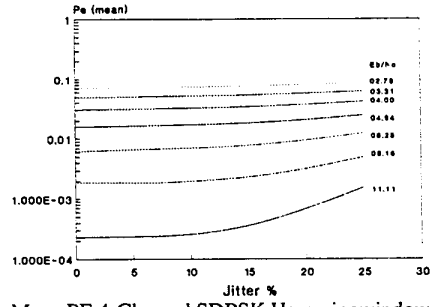

Figure-16: Mean PE,4-Channel SDPSK,Hammingwindow.

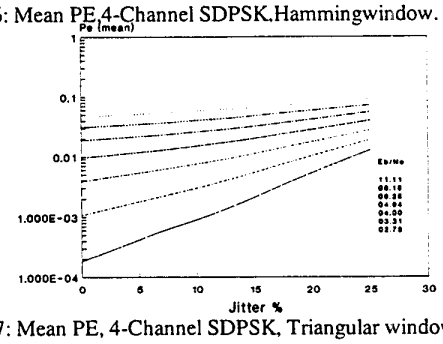

Figure-17: Mean PE, 4-Channel SDPSK, Triangular window.

9.0 Conclusions

In this paper a new nocoherent modulation/demodulation technique is proposed. The suggested approach, SDPSK, is shown to have the same PE as the optimum DPSK in the absence of SSJ with the added advantage of the modulated signal always containing a fundamental frequency component with a period equal to the symbol duration. This allows the symbol synchronization circuitry to reliably detect the start and end of a symbol, hence reducing the probability of SSJ. Also an economical and compact implementation of the block demodulators for both DPSK and SDPSK are suggested using FFT. Preliminary results testing the demodulators were satisfactory. However further analysis of performance in the presence of SSJ along with the effect of windowing on PE needs to be investigated in more depth.

Reference

[1] G.Proakis,"Digital Communications", Second Edition, McGraw-Hill Book Company, 1989.

[2] R. Ziemer, W. Tranter,"Principles of Communications, Systems, Modulation, and Noise", 3rd Edition, Houghton Mifflin Co., 1990.

[3] G. Proakis, D. Manolakis,"Digital Signal Processing, Principles, Algorithms, and Applications", 2ndEdition, Macmillan 1992.

[4] F. Harris,"On the Use of Windows for Harmonic Analysis with the Discrete Fourier Transform", Proceeding of the IEEE, Vol. 66, No. 1, January 1978, pp. 51-83.

[5] L. Aroian,"The Probability of The Product of Two Normally Distributed Variables", Annals of Math. Stat. Vol. 18, 1947, pp. 265-271.